

# Phylogeny of *Bicyclus* (Lepidoptera: Nymphalidae) Inferred from COI, COII, and EF-1 $\alpha$ Gene Sequences

Antónia Monteiro\*<sup>†</sup> and Naomi E. Pierce\*

\*Museum of Comparative Zoology Labs, Harvard University, Boston, Massachusetts; and <sup>†</sup>Institute of Ecological and Evolutionary Sciences, Leiden University, RA Leiden 2300, The Netherlands

Received April 25, 2000; revised September 25, 2000

Despite the fact that *Bicyclus anynana* has become an important model species for wing-pattern developmental biology and studies of phenotypic plasticity, little is known of the evolutionary history of the genus *Bicyclus* and the position of *B. anynana*. Understanding the evolution of development as well as the evolution of plasticity can be attempted in this species-rich genus that displays a large range of wing patterns with variable degrees of phenotypic responses to the environment. A context to guide extrapolations from population genetic studies within *B. anynana* to those between closely related species has been long overdue. A phylogeny of 54 of the 80 known *Bicyclus* species is presented based on the combined 3000-bp sequences of two mitochondrial genes, cytochrome oxidase I and II, and the nuclear gene, elongation factor 1 $\alpha$ . A series of tree topologies, constructed either from the individual genes or from the combined data, using heuristic searches under a variety of weighting schemes were compared under the best maximum-likelihood models fitted for each gene separately. The most likely tree topology to have generated the three data sets was found to be a tree resulting from a combined MP analysis with equal weights. Most phylogenetic signal for the analysis comes from silent substitutions at the third position, and despite the faster rate of evolution and higher levels of homoplasy of the mitochondrial genes relative to the nuclear gene, the latter does not show substantially stronger support for basal clades. Finally, moving branches from the chosen tree topology to other positions on the tree so as to comply better with a previous morphological study did not significantly affect tree length. © 2000 Academic Press

**Key Words:** *Bicyclus*; Lepidoptera; Nymphalidae; Satyrinae; phylogeny; COI; COII; EF-1 $\alpha$ ; parsimony; maximum likelihood; phenotypic plasticity; wing pattern; development; eyespots.

## INTRODUCTION

The genus *Bicyclus* Kirby, 1871 (Lepidoptera, Nymphalidae, Satyrinae), comprises around 80 spe-

cies, most of which live in continental African forests, with a few found in savanna regions (Condamin, 1973; Larsen, 1999). One species, *B. anynana*, is also found in Madagascar. They are some of the most common forest satyrids, flying slowly in the forest understory and feeding on fermenting fruit. The larvae feed primarily on grasses. The group diversified in mainland Africa probably at the same time as diversification of their food plants, during the Oligocene or Miocene (middle Tertiary), anywhere from 5 to 38 million years ago (Miller, 1968).

In Condamin's extensive and almost complete monograph of the genus (Condamin, 1973), the then-known 77 species were classified into 29 species groups. In most cases, members of a group shared similar characteristics of the male genitalia but, in some cases, only wing shape and wing pattern. The monograph also contains a cladogram showing the relationships between the 29 species groups, but no information about how it was constructed.

The relationships of *Bicyclus* to other genera are currently unresolved. Candidates for sister taxa are grouped within the Mycalesina, a subtribe of the Elymniini, consisting of some 240 species worldwide (Ackery, 1988; Lees, 1997). Of the 11 mycalesine genera, relatives to *Bicyclus* primarily include *Henotesia* Butler, 1879, consisting of around 41 species mostly found in Madagascar, with another 11 species found in mainland Africa, 4 additional genera containing about 16 species found only in Madagascar (*Masoura* Hemming, 1964; *Admiratio* Hemming, 1964; *Houlbertia* Oberthur, 1916; and *Heteropsis* Westwood, 1850); *Hallelesis* Condamin, 1961, with 2 West African species; and the oriental genus *Mycalesis* Hübner, 1818, with about 87 species (Aoki *et al.*, 1982).

Lees (1997) found limited morphological evidence supporting monophyly of the five Madagascan genera, although taxon sampling of African genera was not dense enough to settle this issue. The remaining three mycalesine genera (*Orsotriaena* Wallengren, 1858; *Lohora* Moore, 1880; and *Nirvana*, Tsukada and Nishiyama, 1979) include relatively few species in south-

east Asia and Sulawesi. *Bicyclus* differs from *Henotesia* and *Mycalesis* but not *Hallelesis* by the absence of hairs between the ommatidia in the eyes. It differs from *Hallelesis* by the absence of coremata (tufts of long hairs along the vinculum) in the male genitalia and also by the absence in the males of hair tufts in the A1–A2 interval of the posterior wing (Condamin, 1973).

Over the past 10 years, *B. anynana* has been used as a model in studies of phenotypic plasticity (Brakefield and Reitsma, 1991; Windig *et al.*, 1994; Brakefield, 1996; Roskam and Brakefield, 1996; Brakefield *et al.*, 1998), conservation genetics (Saccheri *et al.*, 1996, 1999), wing-pattern development (French and Brakefield, 1992, 1995; Brakefield and French 1995, 1999; Monteiro *et al.*, 1994, 1997a,b,c; Brakefield *et al.*, 1996; Brakefield, 1998), and also life history evolution (Brakefield and Kesbeke, 1997). From an evolutionary perspective, all these areas benefit from comparative studies of closely related species. For this purpose, a robust phylogeny of the genus was needed.

Here we present the molecular phylogeny of 54 *Bicyclus* species constructed with two mitochondrial genes, cytochrome oxidase I and II, and one nuclear gene, elongation factor 1 $\alpha$  (EF-1 $\alpha$ ). We chose these genes because of their proven utility in several studies within the Lepidoptera. In particular, a mtDNA segment (950 bp) spanning parts of COI and COII produced a well-resolved tree for 37 species of *Heliconius* butterflies and could even separate eastern and western races within *H. erato* (Brower, 1994a,b). COI and COII were useful in fully resolving topologies within species of the lycaenid genera *Jalmenus* (Pierce and Nash, 1999) and *Chrysoritis* (Rand *et al.*, 2000), as well as within groups of the genus *Papilio* (Caterino and Sperling, 1999). Reed and Sperling (1999) found that including EF-1 $\alpha$  further resolved relationships among species groups within the same genus. EF-1 $\alpha$  was also useful in resolving clades at subfamily rank and lower, in major groups of the Noctuoidea (arising probably in the early Tertiary; Cho *et al.*, 1995, Mitchell *et al.*, 1997).

We sought evidence from multiple genes so as to (1) identify blatant experimental errors in sequencing; (2) sample separate nuclear and mitochondrial gene trees with different inheritance properties and coalescence times, thus helping to distinguish species trees from gene trees (Maddison, 1997); and (3) utilize genes evolving at different rates to improve the phylogenetic signal at different levels of divergence.

## MATERIAL AND METHODS

Forty *Bicyclus* species were caught using hand nets and fruit traps in the forests of Uganda and Cameroon in July 1997 and February 1998. Upon collection, the

wings were separated from the body and stored in glassine envelopes and the bodies were preserved in 100% ethanol. An additional 18 species were caught by other researchers and collaborators and were between 1 and 4 years old at the time of DNA extraction (Table 1). These were either preserved dry in glassine envelopes or in 100% ethanol.

We sampled three individuals from different populations of *B. safitza* (Uganda, South Africa, and Malawi) to estimate intraspecific versus interspecific molecular divergence. Sampling of the *Bicyclus* genus covered all but two monospecific species groups as defined by Condamin (1973), containing *B. similis* and *B. nobilis*.

As outgroups we used two *Henotesia* species found in mainland Africa (*H. peitho* and *H. perspicua*), *Hallelesis asochis* and *Mycalesis francisca*. Representatives from each of these genera were used solely to provide a root for the topology of the putative ingroup and were included in the analysis without an *a priori* assumption regarding their outgroup status. We offer no assessment of relationships among them here. In total, 58 species and 60 specimens were used for the phylogenetic analysis.

DNA was extracted from tissue in the suitable first to third abdominal segments by mechanical trituration of the tissue (in buffer solution), followed by 1 h of chemical digestion with proteinase K and then a salt and ethanol precipitation. DNA was stored in TE buffer at  $-20^{\circ}\text{C}$ . For one of the dry specimens, *B. anisops*, DNA was extracted from the wing hinge tissue and dried wing androconial cells. Amplification of DNA was done using two methods: a direct method using primers that amplified a sequence around 500 bp in length and a nested method using a sequence of primers that first amplified a large piece of around 1000 bp and then amplified a smaller 500-bp fragment from each half of the larger piece.

Parts of cytochrome oxidase I and II (COI and COII) were sequenced using the primer combinations listed in Table 2. For the nested method, for instance with COI, the primer sets "Ron" and "Hobbes" were first used to amplify a large gene product. This product was used as template for the second amplification reaction, done with either "Ron/Nancy" or "Tonya/Hobbes" primer combinations. This procedure tended to yield a large quantity of the target DNA fragment for direct sequencing.

PCR products were cleaned using QIAquick, by Qiagen, PCR purification columns when only one DNA band was visible on a gel, or, when more than one band was present, a combination of gel-separation and subsequent purification with QIAquick gel extraction columns. Sequencing reactions were done using a Perkin-Elmer dye terminator cycle sequencing kit. Both DNA strands of the ca. 500-bp fragments were sequenced in an ABI 370 automated sequencer. Sequences of COI and COII were aligned against sequences from *Dro-*

**TABLE 1**  
**Species List, Museum Sample Accession Number of Specimens Used for DNA Analysis, and Collectors/Suppliers of Specimens**

Species	Sample accession number at MCZ	Location	Collector <sup>a</sup>
<i>B. alboplagus</i>	AM-98-V218	Congo	RD (e)
<i>B. analis</i>	AM-98-R023	Cameroon, Dja Reserve	AM (e)
<i>B. anisops</i>	AM-98-A3	Cameroon, Mt. Camerron	HR (d)
<i>B. angulosus</i>	AM-97-W242	Uganda, Budongo Forest	AM (e)
<i>B. anynana</i>	AM-97-V725	The Netherlands <sup>b</sup>	AM (e)
<i>B. auricrudus</i>	AM-97-V177	Uganda, Kibale Forest	AM (e)
<i>B. buea</i>	AM-97-V200	Uganda, Kibale Forest	AM (e)
<i>B. campus</i>	AM-97-W245	Uganda, Budongo Forest	AM (e)
<i>B. cottrelli</i>	AM-98-R101	Malawi, Zomba	JW/PB (d)
<i>B. dentatus</i>	AM-97-V179	Uganda, Kibale Forest	AM (e)
<i>B. dorothea</i>	AM-98-R936	Cameroon, Dja Reserve	AM (e)
<i>B. dubius</i>	AM-97-W231	Uganda, Bwindi	AM (e)
<i>B. ena</i>	AM-98-R089	Malawi, Zomba	JW/PB (d)
<i>B. evadne</i>	AM-98-R035	Cameroon, Dja Reserve	AM (e)
<i>B. funebris</i>	AM-97-W232	Uganda, Bwindi	AM (e)
<i>B. golo</i>	AM-98-R949	Cameroon, Dja Reserve	AM (e)
<i>B. graueri</i>	AM-97-W219	Uganda, Kibale Forest	AM (e)
<i>B. hewitsoni</i>	AM-98-R966	Cameroon, Dja Reserve	AM (e)
<i>B. hyperanthus</i>	AM-97-W228	Uganda, Bwindi	AM (e)
<i>B. iccius</i>	AM-98-R022	Cameroon, Dja Reserve	AM (e)
<i>B. ignobilis</i>	AM-97-V227	Congo	RD (e)
<i>B. istaris</i>	AM-97-V165	Uganda, Kibale Forest	AM (e)
<i>B. italus</i>	AM-98-R031	Cameroon, Dja Reserve	AM (e)
<i>B. jefferyi</i>	AM-97-V168	Uganda, Kibale Forest	AM (e)
<i>B. kenia</i>	AM-98-R079	Kenya, Meru	TL (d)
<i>B. madetes</i>	AM-98-R065	Cameroon, Dja Reserve	AM (e)
<i>B. mandanes</i>	AM-97-V183	Uganda, Kibale Forest	AM (e)
<i>B. matuta</i>	AM-98-V911	Congo	RD (e)
<i>B. medontias</i>	AM-98-R987	Cameroon, Dja Reserve	AM (e)
<i>B. mesogenus</i>	AM-97-V189	Uganda, Kibale Forest	AM (e)
<i>B. mollitia</i>	AM-97-V184	Uganda, Kibale Forest	AM (e)
<i>B. moyses</i>	AM-98-R942	Cameroon, Dja Reserve	AM (e)
<i>B. pavonis</i>	AM-98-R067	Ghana, Anfoega	TL (e)
<i>B. persimilis</i>	AM-98-V898	Congo, Butuhe	RD (e)
<i>B. procorus</i>	AM-97-V909	Congo	RD (e)
<i>B. safitza U</i>	AM-97-V211	Uganda, QENP	AM (e)
<i>B. safitza M</i>	AM-98-R096	Malawi, Zomba	JW/PB (d)
<i>B. safitza SA</i>	DR-98-U575	South Africa, Tsitsikamma	DR (e)
<i>B. sambulos</i>	AM-98-R989	Cameroon, Dja Reserve	AM (e)
<i>B. sanaos</i>	AM-98-R088	Nigeria, Oban Hills	TL (d)
<i>B. sandace</i>	AM-97-W239	Uganda, Budongo Forest	AM (e)
<i>B. sangmelinae</i>	AM-98-X980	Ghana	TL (e)
<i>B. sciathis</i>	AM-98-R016	Cameroon, Dja Reserve	AM (e)
<i>B. sebetus</i>	AM-98-R968	Cameroon, Dja Reserve	AM (e)
<i>B. smithi</i>	AM-97-V187	Uganda, Kibale Forest	AM (e)
<i>B. sophrosyne</i>	AM-97-W220	Uganda, Kibale Forest	AM (e)
<i>B. sweatneri</i>	AM-98-V224	Congo	RD (e)
<i>B. taenias</i>	AM-98-R024	Cameroon, Dja Reserve	AM (e)
<i>B. technatis</i>	AM-98-R964	Cameroon, Dja Reserve	AM (e)
<i>B. trilophus</i>	AM-98-R036	Cameroon, Dja Reserve	AM (e)
<i>B. uniformis</i>	AM-98-R004	Cameroon, Dja Reserve	AM (e)
<i>B. vansonii</i>	AM-98-R092	Malawi, Zomba	JW/PB (d)
<i>B. vulgaris</i>	AM-97-W236	Uganda, Bwindi	AM (e)
<i>B. xeneas</i>	AM-98-R038	Cameroon, Dja Reserve	AM (e)
<i>B. xeneoides</i>	AM-97-V234	Congo	RD (e)
<i>B. zinebi</i>	AM-98-R087	Nigeria, Oban Hills	TL (d)
<i>Hallelesis asochis</i>	AM-98-R044	Cameroon, Dja Reserve	AM (e)
<i>Henotesia peitho</i>	AM-97-W253	Uganda, Kibale Forest	AM (e)
<i>Henotesia perspicua</i>	AM-97-V215	Uganda, QENP	AM (e)
<i>Mycalesis francisca</i>	AM-98-R086	Japan, Mt. Shizuhata	DL (e)

*Note.* All specimens are deposited at the Museum of Comparative Zoology, Harvard University. Bodies are stored in 100% ethanol at -80°C, and wings are stored dry in glassine envelopes.

<sup>a</sup> AM, Antónia Monteiro; DL, David Lees; DR, Doug Rand; HR, Hans Roskam; JW, John Wilson; PB, Paul Brakefield; RD, Robert Ducarme; TL, Torben Larsen. (e) and (d), ethanol or dry preservation at time of collection.

<sup>b</sup> From a lab stock established from 80 females collected in Malawi in 1988.

**TABLE 2**  
**Primers Used in the Amplification of COI, COII, and EF-1 $\alpha$**

Gene	Name of primer (forward or reverse reading) and position	Sequence of primer	Max/Min length (bp) of sequenced product <sup>a</sup>
COI	Ron (f)—1730 Nancy (r)—2217	GGA TCA CCT GAT ATA GCA TTC CC CCC GGT AAA ATT AAA ATA TAA ACT TC	479/325
	Tonya (f)—2192 Hobbes (r)—2757	GAA GTT TAT ATT TTA ATT TTA CCG GG AAA TGT TGN GGR AAA AAT GTT A	536/424
	Ron/Hobbes		≈1000
COII	George(I) (f)—2774 Phyllis—3298	ATA CCT CGA CGT TAT TCA GA GTA ATA GCI GGT AAR ATA GTT CA	488/241
	Strom (f)—3271 Eva (r)—3799 BtLYS (r)—3808	TAA TTT GAA CTA TYT TAC CIG C GAG ACC ATT ACT TGC TTT CAG TCA TCT GTT TAA GAG ACC AGT ACT TG	511/416
	George/Eva		≈1000
	George/BtLYs		≈1000
EF-1 $\alpha$	ef44 (f)—240 ef51r (r)—650	GCY GAR CGY GAR CGT GGT ATY AC CAT GTT GTC GCC GTG CCA AC	401/332
	ef51.9 (f)—798 efrcM4 (r)—1351	CAR GAC GTA TAC AAA ATC GG ACA GCV ACK GTY TGY CTC ATR TC	520/422
	ef44/efrcM4		≈1000

*Note.* Primer positions are given relative to published sequences of *Drosophila yakuba* (whole mRNA) and *Bombyx mori* (EF-1 $\alpha$ ).

<sup>a</sup> In the following species we could not amplify and/or sequence some of the gene fragments: Ron/Nancy (*B. ena*); Tonya/Hobbes (*B. ena*, *B. uniformis*); George/Phyllis (*B. anisops*, *B. sangmelinae*, *B. sweadneri*, *B. vansonii*); Strom/Eva/BtLYS (*B. alboplagus*, *B. anisops*, *B. hyperanthus*, *B. ignobilis*, *B. sangmelinae*, *B. sweadneri*, *B. technatis*); and ef51.9/efrcM4 (*B. sangmelinae*).

*sophila yakuba* (Clary and Wolstenholme, 1985). Sequences of EF-1 $\alpha$  were aligned against one of *Bombyx mori* (Kamiie *et al.*, 1993). Alignments were automated using Sequencher 3.0. Analysis were performed in PAUP\*, version 4.0b2a (Swofford, 1998), and MacClade, version 3.06 (Maddison and Maddison, 1992). Measures of synonymous versus nonsynonymous substitutions were calculated using the Nei and Gojobori (1986) method, implemented in the program MEA, Molecular Evolutionary Analysis, generously provided by the author, E. Moriyama.

#### Phylogenetic Analysis

For the purposes of phylogenetic analysis we decided to partition the data into blocks containing (independently amplified) primer-pair partitions rather than strictly respecting true gene boundaries. In particular, the "COI" gene partition only contains bases from the COI gene; the "COII" partition contains approximately the first 200 bases from COI and also contains the tRNA for leucine; and all "EF-1 $\alpha$ " bases correspond to the EF-1 $\alpha$  gene. When analyzing codon positions within the COII partition, the tRNA bases were not included.

The chosen analysis procedure took the following seven steps:

1. We tested whether the three gene data sets were combinable using the Partition Homogeneity Test as implemented in PAUP\* 4.0b2 and described by Farris *et al.* (1994) as the incongruence length difference (ILD) test. We implemented the test under parsimony with closest taxa addition and no swapping and used 1000 replicates to generate the null distribution of tree lengths. Since four species were not sequenced fully for all three genes, these were first removed from the partition test, so as to make tree lengths comparable.

2. We built equally weighted maximum-parsimony (MP) trees for each gene separately.

3. We built equally weighted MP trees for the combined data.

4. Under the assumption that slower evolving positions/genes have lower degrees of homoplasy than faster evolving ones, and that certain base changes (transversions) occur less often than others (transitions), and hence are more likely to retrieve correct groupings of species, we tried a series of weighting schemes: first and second positions were weighted more heavily, relative to third positions; transversions were weighted more heavily relative to transversions; all bases in the slower evolving nuclear gene were given a higher weight relative to those in the mitochon-

drial genes; and several combinations of these weighting schemes were applied together. Appropriate positional weights and character-change weights were estimated using maximum likelihood (ML), on one of the MP tree topologies from the combined data (Swoford *et al.*, 1996).

To measure how fast each gene was evolving we used branch length information from the initial MP analysis performed on the separate genes (step 2). In particular, we took the branch lengths of pairs of tip species that were closely related in all the three separate analyses. This use of closely related species alone gives us the best estimate of the real rates of evolution with hopefully little effect from saturation (Moriyama and Powell, 1997). For each gene, the branch lengths were summed across all species pairs.

5. To compare all the tree topologies generated so far we used a ML criterion. We took the first tree topology obtained under the equal weighted MP combined analysis (as in step 3) and pruned from this tree the 4 species that were not sequenced for all of the three genes. Then, on the pruned tree, we estimated the best-fitting ML model for each gene separately. We tried a succession of models, from the simple Jukes and Cantor model to the general time reversible (GTR) model, assuming a  $\gamma$  distribution (G) of rate heterogeneity across sites, a proportion of invariable sites (I), and unequal base frequencies. Successively more complex models were tested for a significantly better fit using the likelihood ratio test (LRT).

6. We evaluated each of the previous combined data MP tree topologies under the best ML models found in step 5. Each tree topology was given a likelihood score under each gene's best-fitting model and the likelihood scores were summed across genes to obtain an overall likelihood fit of the data to the topology for all three genes simultaneously. The topologies were each fitted twice: once using parameters estimated for each gene from a single, global tree (the same tree as in step 3, using parameters from step 5), and once using parameters estimated for each gene on the MP tree topology under evaluation. The topology for which the sum of the likelihoods for all three genes was highest was deemed the "best" topology. It was the topology that, most likely, gave rise to the combined data.

ML allowed us to compare tree topologies with very different tree lengths (due to the different weighting schemes applied). We did not apply likelihood as the criterion to search for alternative tree topologies, as under PAUP\* there is still no possibility of constructing a combined gene ML model if the genes in question have different base frequencies (which was the case here, with the mitochondrial genes being AT rich). For the same reason, ML models used to evaluate alternative tree topologies were developed for each gene independently rather than for the combined data set.

7. In order to calculate saturation curves for each

**TABLE 3**  
**Type and Number of Molecular Characters Analyzed for Each Gene**

Gene	COI	COII	EF-1 $\alpha$
Total number of analyzed characters	945	969	890
Number of parsimony-informative characters	318 (33.7%)	288 (29.7%)	169 (19.0%)
First position	52	65	10
Second position	15	11	2
Third position	251	201	157
Number of variable but parsimony-uninformative characters	57 (6.0%)	86 (8.9%)	78 (8.8%)
First position	20	27	9
Second position	10	18	7
Third position	27	39	62
Number of constant characters	570 (60.3%)	595 (61.4%)	643 (72.2%)
First position	243	208	277
Second position	290	269	288
Third position	37	59	78

gene, we plotted the uncorrected pairwise "p" divergences against pairwise divergences corrected by the ML parameter estimates from each gene's best-fitting model. To compare the degree of homoplasy for each gene, Bezier curves were fitted to the data by eye and compared.

## RESULTS

According to the ILD test, partitions of the data into COI, COII, and EF-1 $\alpha$  are homogeneous (sum of gene tree lengths = 4413;  $P = 0.817$ ). COI and COII gene partitions alone are homogeneous (sum of gene tree lengths = 3765;  $P = 0.087$ ) and partitions between COI and COII together and EF-1 $\alpha$  are also homogeneous (sum of tree lengths = 4596,  $P = 0.613$ ).

COI showed the highest number of parsimony-informative characters, followed closely by COII. EF-1 $\alpha$  displayed the highest number of constant characters and the smallest number of parsimony-informative characters (Table 3). Most changes occurred at third positions for all three genes. EF-1 $\alpha$  had 93% of its parsimony-informative characters occurring at third positions, relative to 79 and 73% in COI and COII, respectively.

Using the test of homogeneity of base composition implemented in PAUP\*, we found no heterogeneity in base composition across species when all codon positions were analyzed together (Table 4). However, when base composition was broken down by codon position, we found significant base heterogeneity across species for COI third positions. When such heterogeneity is

**TABLE 4**  
**Base Composition Broken Down by Codon Position**

Gene	Empirical base frequencies				$\chi^2$ test statistic ( $df = 177$ )	P value
	A	C	G	T		
COI						
All positions	0.30	0.16	0.14	0.39	53.87	1.00
First position	0.31	0.15	0.26	0.29	24.47	1.00
Second position	0.18	0.25	0.16	0.42	8.98	1.00
Third position	0.41	0.10	0.01	0.48	216.33	0.02*
COII						
All positions	0.34	0.14	0.10	0.42	42.70	1.00
First position	0.37	0.16	0.15	0.32	35.75	1.00
Second position	0.29	0.18	0.12	0.41	25.05	1.00
Third position	0.38	0.07	0.01	0.54	120.34	0.99
EF-1 $\alpha$						
All positions	0.25	0.27	0.23	0.24	21.34	1.00
First position	0.29	0.18	0.39	0.15	6.77	1.00
Second position	0.31	0.27	0.14	0.28	6.11	1.00
Third position	0.16	0.38	0.17	0.28	56.89	1.00

*Note.* Heterogeneous base composition across species was tested with a  $\chi^2$  test statistic.

present, species can group together under MP due to similarity of base composition rather than phylogenetic signal (Chang and Campbell, 2000). We looked at this effect by examining whether the species with the highest A, C, G, or T content were clustered together in the COI tree and also by comparing tree topologies constructed with and without third codon positions from COI (see below).

MP analysis using equal weights produced 19 MP trees for COI of length 2039 (Fig. 1), 8 MP trees for COII with length 1656 (Fig. 1), and 8050 MP trees for EF-1 $\alpha$  of length 774 (Fig. 1). The combined data analysis produced 5 MP trees of length 4559 (Trees 1–5; Fig. 2).

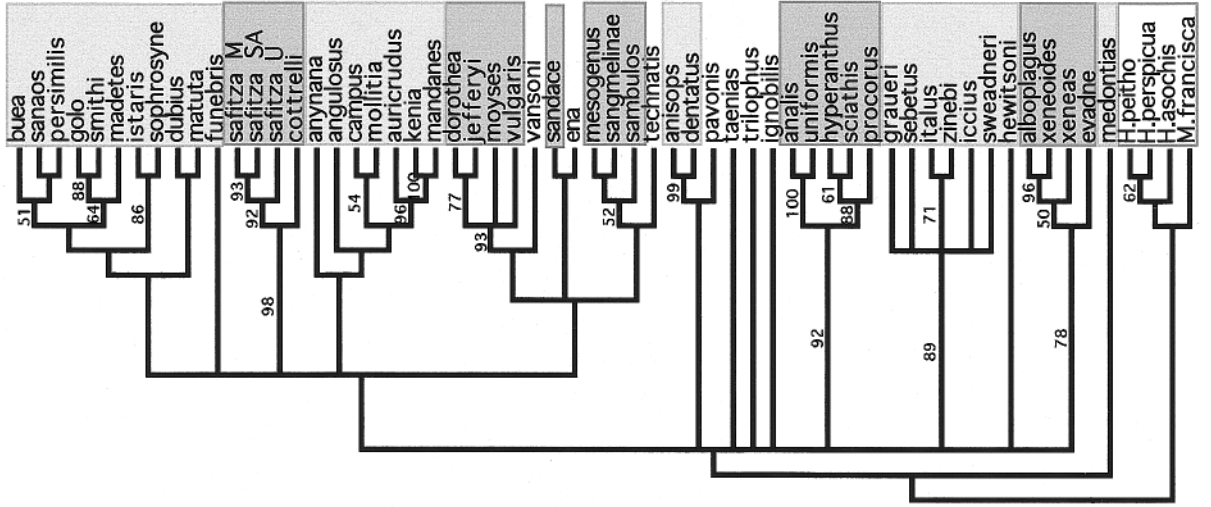
To test whether base heterogeneity at COI third positions was affecting tree topology, we compared the combined data analysis consensus tree (Fig. 2A) with a consensus tree produced from all genes excluding COI third positions (not shown). This latter search produced 8 MP trees with an identical topology to the tree containing all bases, with the exception that the *istaris-sophrosyne* clade clustered first with the *buea-sanaos-persimilis* clade, rather than with the *golo-smithi-madetes* clade. This clustering, however, was only supported by a bootstrap value of 56%. The other differences were that the clade that starts with *mesogenus* and ends with *technatis* (Fig. 2A) was now supported with a bootstrap value of 75%. Other nodes in the tree, however, lost bootstrap support, including two basal nodes that had bootstrap values of 58 and 82% (Fig. 2A). Also, by examining the top 10 species with the highest and lowest A, C, G, or T content, we could find no particular association of clusters of species with similar base frequencies and clades on the phylogenetic estimate (Fig. 2A). In all cases, these top 10

species belonged to several species groups, scattered across the tree. These two results led us to believe that base heterogeneity at COI third positions does not significantly influence the topology obtained under MP with the combined data.

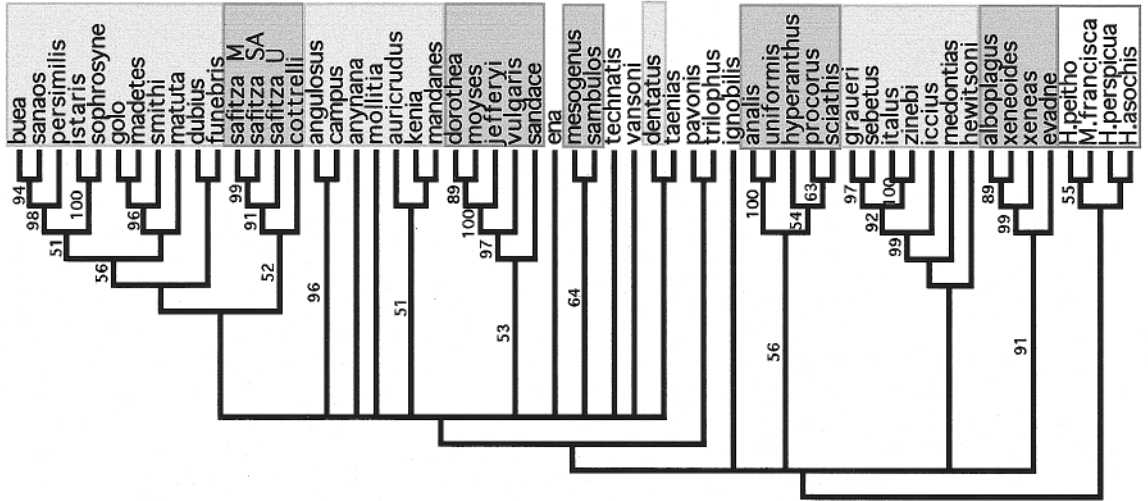
We compared the utility of each gene in resolving relationships among species by comparing the independently derived tree topologies and bootstrap support estimates of several clades (Fig. 1). COI was the only gene that identified the *alboplagus-evadne* clade as the most basal (but with no strong bootstrap support), and it was also the gene showing greater resolution in another basal clade, the *graueri-hewitsoni* clade (see clade branching order in the phylogram of Fig. 5). EF-1 $\alpha$  showed slightly higher support for a second basal clade (the *nalis-procorus* clade), relative to COI. On the other hand, COI and COII resolved more tip nodes and on average had higher bootstrap support for these nodes relative to EF-1 $\alpha$ .

To test for the utility of the phylogenetic signal at first, second, and third positions, we conducted one combined data, MP search, based only on first and second positions and another based only on third positions (not shown). When all third positions were excluded, we obtained a consensus of 18 MP trees, with good bootstrap support only at tip clades, with the exception of the most basal node (separating the ingroup from the outgroups) that had 88% bootstrap support. A search using only third positions, however, produced a consensus of 3 MP trees, with higher bootstrap support and better supported nodes toward the base of the tree, relative to the previous search. The node for the ingroup, however, had lower support (54%) than that obtained from first and second positions alone. All the well-supported clades (with bootstrap

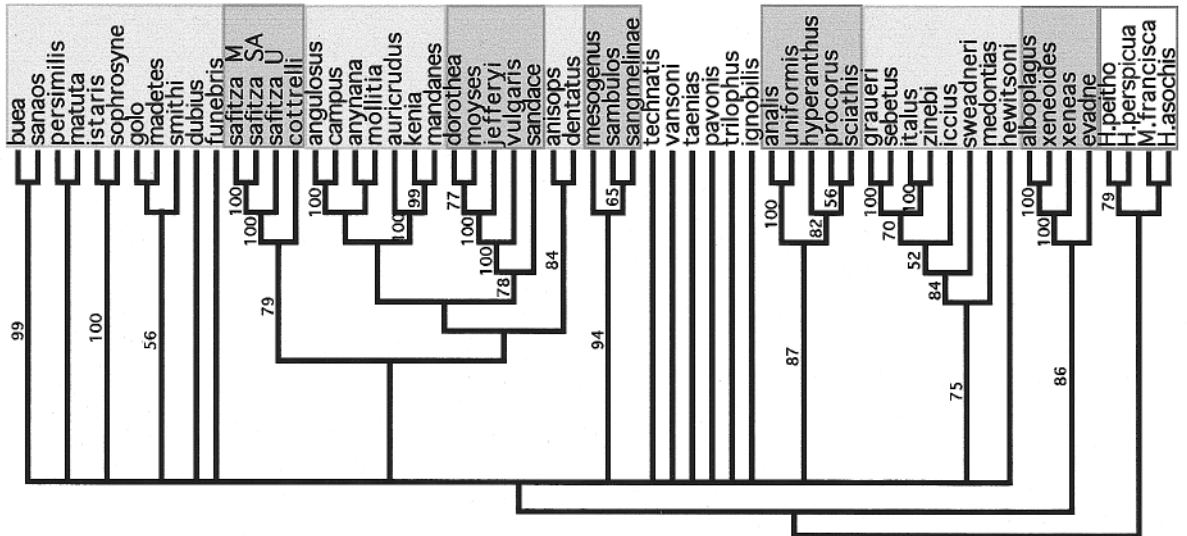
EF-1a

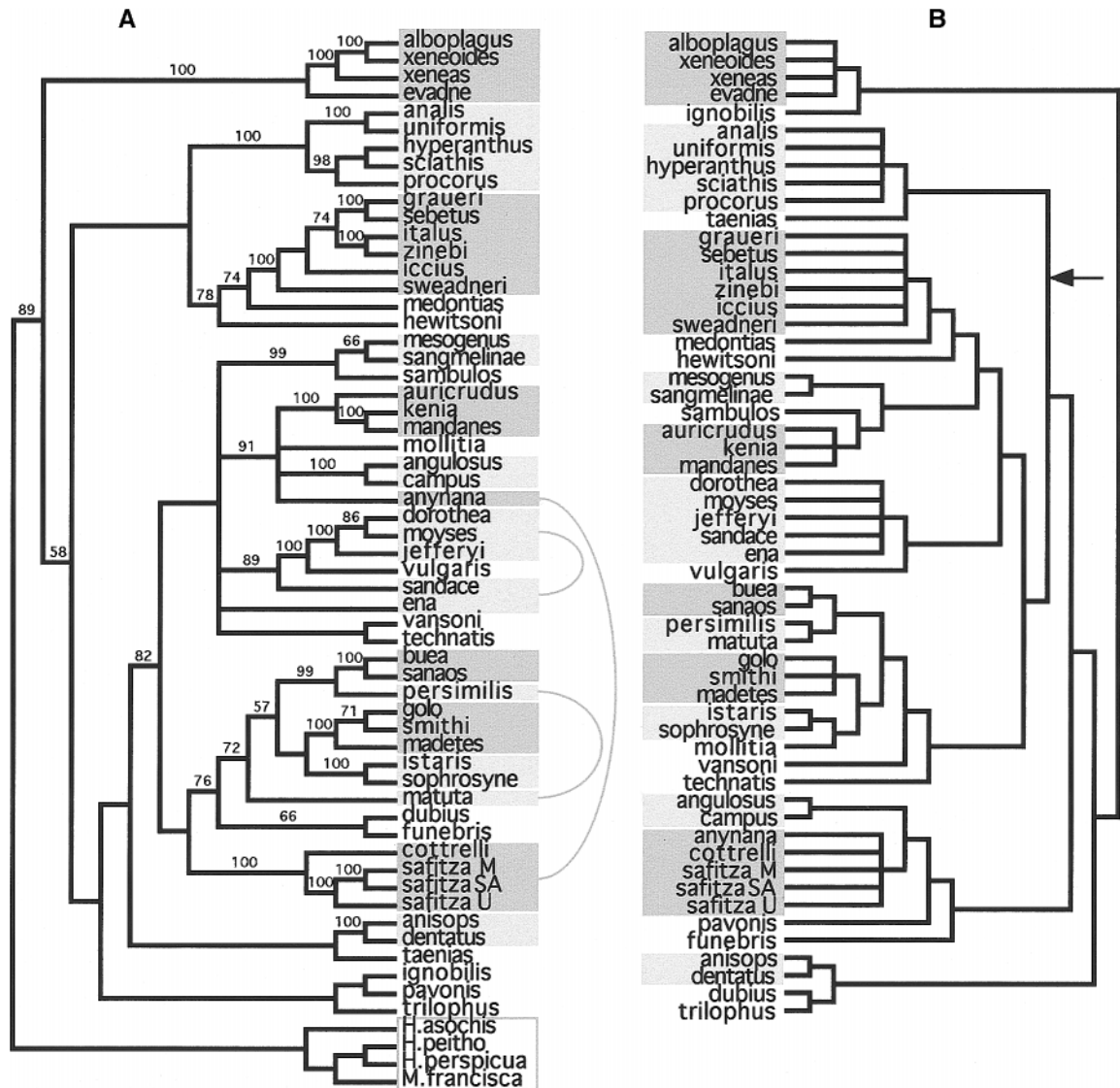


COII



COI





**FIG. 2.** (A) Strict consensus tree from a MP analysis with equal weights for the combined data set. Bootstrap values from 1000 resamplings from the entire data set are shown above tree branches. Shaded blocks highlight members of species groups as defined by the morphological study of the genus by Condamin (1973). Species not shaded either are members of monospecific groups or were the only members sampled from the group in this study. Members of the same species group that were separated on this phylogeny are indicated via a connecting arch. Outgroup taxa are grouped in a clear box. (B) Condamin's morphological cladogram pruned to show only sequenced taxa and rerooted to comply with the root found in the molecular analysis (the location of the root postulated by Condamin is shown with an arrow).

values >50%) in both searches were congruent with those of Fig. 2A.

When base positions were converted to amino acids (and the tRNA leucine was excluded), several thousand topologies produced MP solutions. There was good bootstrap support for the ingroup (78%), but no support

for the most basal nodes within *Bicyclus*. All the well-supported nodes (18 vs 38 with the untranslated data) were congruent with those in Fig. 2A.

From the comparison of instantaneous rates of evolution from 11 pairs of tip species (Table 5), and taking all changes in consideration (but excluding those in the

**FIG. 1.** Strict consensus trees from MP analysis with equal weights performed for each gene separately. COI shows the consensus tree from 19 MP trees, COII from 8 MP trees, and EF-1 $\alpha$  from 8050 MP trees. Bootstrap values from 100 resamplings from the data (a tree search for each bootstrap sample involved a heuristic search with the starting tree produced by 10 random addition sequences (TBR was used to swap branches)) are displayed above branches. Shaded blocks represent clades of species that were well supported (with bootstrap values above 75%) in the combined data analysis (Fig. 2A). Outgroup taxa are grouped in clear boxes.



TABLE 5

**Partition Parameters Estimated from the Sum of the Branch Lengths between Pairs of Tip Species on One MP Tree from Each Gene, Chosen at Random**

Gene	Position	Total No. of substitutions	No. of sites compared	No. substitutions/site	Relative substitution rate <sup>a</sup>	Average rate of substitutions/site across species pairs	
						Synonymous	Nonsynonymous
COI	First	43	315	0.14	0.45	0.1546	0.0013
	Second	7	315	0.02	0.07		
	Third	321	315	1.02	3.35		
	All	371	945	0.39	3.75		
COII	First	28	298	0.09	0.31	0.1700	0.0051
	Second	12	298	0.04	0.13		
	Third	248	298	0.83	2.74		
	All	288	894	0.32	3.08		
EF-1 $\alpha$	First	3	296	0.01	0.03	0.0367	0.0003
	Second	0	296	0.00	0.00		
	Third	90	296	0.30	1.00		
	All	93	888	0.10	1.00		

*Note.* Synonymous and nonsynonymous rates were obtained from pairwise comparisons of nucleotide sequences. The pairs of species used were xeneoides/xeneas; procorus/sciathis; mesogenus/sambulos; buea/sanaos; istaris/sophrosyne; golo/madetes; kenia/mandanes; dorothea/moyeses; safitza\_M/cottrelli; graueri/sebetus; italus/zinebi.

<sup>a</sup> Relative to EF-1 $\alpha$  third positions, arbitrarily set to one, or to all positions in EF-1 $\alpha$ .

tRNA leucine), we found COI and COII to be evolving 3.8 and 3 times faster than EF-1 $\alpha$ , respectively. The average rate of synonymous substitutions/site was approximately 4.5 times higher in the mitochondrial genes relative to the nuclear gene. COI third positions alone are evolving 3.4 times faster than those of EF-1 $\alpha$ , whereas those in COII are evolving 2.8 times faster. EF-1 $\alpha$  is the slowest evolving gene not only due to a larger number of constant characters (see Table 3), which could arise due to functional constraints, but also because it has lower rates of nucleotide substitutions. COII seems to be less functionally constrained relative to COI, due to a slightly higher rate of nonsynonymous substitutions (at second positions). COI is evolving faster than COII mostly due to a higher substitution rate at first and third positions.

Using the first of the five MP trees from the equally weighted combined analysis (Tree 1), we calculated the best-fitting ML model for that tree topology for each gene separately (see Tables 6 and 7). Likelihood ratio tests done between the model with the highest likelihood and the other models with fewer free parameters but lower likelihoods indicated that the best-fitting model for the three genes was the most complex, i.e., a GTR model assuming a proportion of invariable sites (I) and a  $\gamma$  parameter (G). However, for EF-1 $\alpha$  this model was not significantly better than GTR + I + G, assuming equal base frequencies, with three fewer parameters, and this model was the chosen model for this gene in subsequent analysis.

Saturation curves for the three genes (Fig. 3) showed that EF-1 $\alpha$  displayed a lower degree of homoplasy relative to COI and COII because the curve of best fit to

the data was closest to the  $x = y$  line over all pairwise comparisons. However, the number of potentially informative sites present in EF-1 $\alpha$ , as measured by the maximum values of uncorrected “ $p$ ” pairwise divergences, was almost half of that for COI. Corrected pairwise divergences were almost three times lower than those for COI and COII. EF-1 $\alpha$ , despite having a considerably lower rate of evolution and lower levels of saturation, seems to be most useful at resolving among the tips of the tree, just like the mitochondrial genes (Fig. 1).

All tree topologies estimated under MP, with equal weights and different weighting schemes, were evaluated using the single criterion of ML. In Table 8 we show the five tree topologies with the highest likelihood, which correspond to the five MP trees generated with the combined data equally weighted. All topologies generated with differently weighted codon positions, genes, and/or character changes ( $T_i/T_v$ ), had significantly lower likelihoods relative to the topologies generated with all characters weighted equally (the best weighted topology had a ln likelihood value of 25 points below that of the best tree topology). The tree found with the highest likelihood was Tree 1.

Doubt remained, however, about whether our analysis was suffering from circularity because ML parameters were estimated for each of the genes using the same tree (Tree 1) that ultimately resulted in the highest likelihood sum. However, according to Yang *et al.* (1994), parameter estimates for ML are fairly stable across tree topologies as long as the trees are not “too wrong.”

To be more certain, we decided to check whether different starting tree topologies would give different

TABLE 6

**Different Maximum-Likelihood Models That Were Fitted to the Three Genes Independently Using One of the Most Parsimonious Trees from the Combined Data Set as the Given Tree Topology**

Model	–ln L COI	LRT COI	–ln L COII	LRT COII	–ln L EF-1 $\alpha$	LRT EF-1 $\alpha$	$\chi^2$ critical <sup>a</sup>	df
JC	12,233.44	5245.68	10,768.52	4500.44	6102.02	1882.60	18.31	10
F81	11,968.01	4714.82	10,493.72	3950.84	6057.54	1793.64	14.07	7
K2P	11,729.40	4237.60	10,308.06	3579.52	5819.09	1316.74	16.92	9
HKY85	11,480.30	3739.40	9,996.00	2955.40	5777.91	1234.38	12.59	6
GTR	11,202.35	3183.50	9,874.57	2712.54	5712.13	1102.82	5.99	2
JC + I	10,919.05	2616.90	9,760.07	2483.54	5589.83	858.22	16.92	9
JC + G	10,735.16	2249.12	9,556.96	2077.32	5546.28	771.12	16.92	9
JC + I + G	10,654.31	2087.42	9,518.87	2001.14	5501.21	680.98	15.51	8
F81 + I	10,587.18	1953.16	9,444.87	1853.14	5532.57	743.70	12.59	6
K2P + I	10,398.94	1576.68	9,285.72	1534.84	5298.80	276.16	15.51	8
F81 + G	10,320.26	1419.32	9,194.33	1352.06	5483.56	645.68	12.59	6
F81 + I + G	10,237.55	1253.90	9,148.76	1260.92	5433.39	545.34	11.07	5
K2P + G	10,202.55	1183.90	9,072.55	1108.50	5252.88	184.32	15.51	8
K2P + I + G	10,112.22	1003.24	9,030.30	1024.00	5204.41	87.38	14.07	7
HKY85 + I	9,995.10	769.00	8,885.76	734.92	5282.55	243.66	11.07	5
GTR + I	9,916.15	611.10	8,848.45	660.30	5253.51	185.58	3.84	1
HKY85 + G	9,744.05	266.90	8,611.17	185.740	5237.75	154.06	11.07	5
GTR + G	9,686.20	151.20	8,591.04	145.48	5199.89	78.34	3.84	1
HKY85 + I + G	9,656.95	92.70	8,544.44	52.28	5189.87	58.30	9.49	4
GTR + I + G + ebf	9,765.44	309.68	8,795.38	554.16	5161.32	1.20	7.82	3
GTR + I + G	9,610.60	Best	8,518.30	Best	5160.72	Best		

*Note.* LRT, likelihood ratio test; I, model assuming a proportion of invariable; G, model using a  $\gamma$  parameter of rate heterogeneity across sites; ebf, equal base frequencies. All models were compared against the GTR + G + I model with a LRT.

<sup>a</sup> When the test statistic is smaller than the given critical value of the  $\chi^2$  distribution (for  $P = 0.05$ ), the two models are not statistically different. Model GTR + G + I + ebf is equivalent to GTR + G + I for EF-1 $\alpha$

ML parameter estimates. We calculated for each of the tree topologies of Table 8 (and also for the weighted topologies not shown) specific ML parameters for each gene, using the same models of evolution as before. The second part of Table 8 gives the results of this second analysis. The best tree topology found was also Tree 1, and the rest of the trees followed in an identical order of  $-\ln$  likelihoods to the one found before. In most cases there was only a difference of 2–3 points in the

sums of the  $-\ln$  likelihoods between the models, thus confirming the remarks of Yang *et al.* (1994).

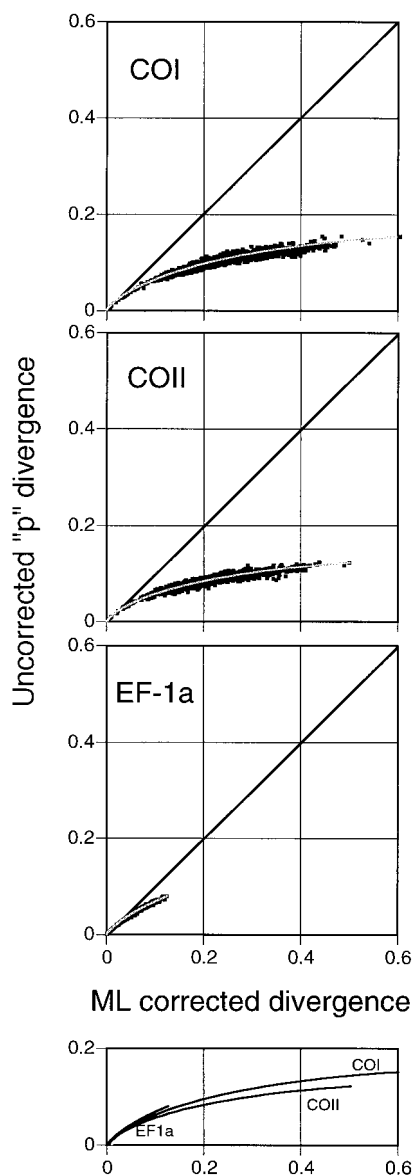
Tree 1 was bootstrapped 1000 times (using all sites; Fig. 4). This yielded good support for the ingroup, *Bicyclus* and for its most basal clade, the *B. alboplagus-evadne* clade. There was lower support for groups at intermediate levels of divergence and strong support for most of the clades at the tips. The three specimens of *B. safitza* always clustered together but interestingly

TABLE 7

**The ML Parameters Estimated for the Best-Fitting Model (GTR + I + G) for Each of the Three Genes, Using the First Most Parsimonious Tree from the Combined Data Set as the Given Tree Topology**

Gene	Estimated % invariable sites	Estimated shape parameter ( $\alpha$ ) from $\gamma$ distribution	Estimated/assumed base frequencies	Estimated instantaneous rate parameters ( $R$ matrix)
COI	54	0.83	A = 0.30 C = 0.14 G = 0.14 T = 0.42	$\mu_a = 6.7$ $\mu_b = 13.0$ $\mu_c = 4.9$ $\mu_d = 0.8$ $\mu_e = 70.1$ $\mu_f = 1$
COII	51	0.55	A = 0.38 C = 0.11 G = 0.06 T = 0.45	$\mu_a = 2.6$ $\mu_b = 11.5$ $\mu_c = 1.1$ $\mu_d = 3.1$ $\mu_e = 35.6$ $\mu_f = 1$
EF-1 $\alpha$	59	0.74	A = 0.25 C = 0.25 G = 0.25 T = 0.25	$\mu_a = 1.1$ $\mu_b = 3.8$ $\mu_c = 2.2$ $\mu_d = 0.7$ $\mu_e = 11.8$ $\mu_f = 1$

*Note.* Model for EF-1 $\alpha$  assumed equal base frequencies.



**FIG. 3.** Scatter plots of uncorrected pairwise divergences versus pairwise divergences corrected by the GTR + I + G maximum-likelihood model fitted for each gene. Bezier curves were fitted by eye to each of the scatter plots and compared against each other in the graph at the bottom.

had longer branches than several other clusters composed of different species. This was especially true of the specimen from Uganda relative to the other two from the neighboring countries of Malawi and South Africa.

Given that the best tree found was Tree 1 (Fig. 4), we tested whether this tree differed significantly from the next best trees with the closest likelihood scores (Trees 4, 3, and 2; see Table 8). When one tree topology is a subset of another more fully resolved tree, then the two hypotheses can be compared with a likelihood ratio test with degrees of freedom equal to the number of additional branches in the more fully resolved tree (Swofford *et al.*, 1996). In our case, however, we only have fully resolved trees and the LRT in a strict sense is invalid. Felsenstein (1988), however, suggested that two trees that differ by a single branch rearrangement can also be compared using the LRT using one degree of freedom.

Tree 1 differs by one branch rearrangement from Trees 2 and 3 (with LRT test statistic = 7; see Table 8) and by two rearrangements from Tree 4. Since the test statistic is higher than the critical value of a  $\chi^2$  with 1 *df* (3.84), we can conclude that Tree 1 is significantly better than Trees 2 and 3. No formal comparison can be made between Tree 1 and Tree 4. Tree 4 has *B. mollitia* move to the base of the *B. angulosus-anyana* clade and the *B. mesogenus-sangmelinae-sambulos* clade move to the base of the *B. angulosus-campus-anyana-mollitia-auricrudus-kenia-mandan* clade.

Finally, we also tested whether Tree 1 or Tree 4 differed significantly from trees with small manual arrangements of particular branches that would comply better with the species groups defined by Condamin (1973). Condamin's species groups are indicated by the shading of blocks in Fig. 2. Whenever a species group consists of only one species (or we happen to have sampled only one species from the group) no shading is applied. In particular there were three instances where members of a species group did not cluster together: (1) *B. persimilis* and *B. matuta*; (2) *B. anyana* with *B. safitza* and *B. cottrelli*; and (3) *B. ena* and *B. sandace* with the *B. dorothea-moses-jefferyi* clade. Because

**TABLE 8**

**Maximum-Likelihood Evaluations of Five Tree Topologies Produced under MP, with Equal Weights**

Tree	Genes	Weights	Tree No./ total	-ln L (COI)	-ln L (COII)	-ln L (EF-1 $\alpha$ )	Sum -ln L	LRT	-ln L (COI)	-ln L (COII)	-ln L (EF-1 $\alpha$ )	Sum -ln L	LRT
1	COI-COII-EF-1 $\alpha$	Equal weights	1/5	9611	8518	5161	23290	Best	9611	8518	5161	23290	Best
2	COI-COII-EF-1 $\alpha$	Equal weights	2/5	9611	8519	5165	23294	7	9611	8519	5165	23294	7
3	COI-COII-EF-1 $\alpha$	Equal weights	3/5	9611	8522	5161	23294	7	9611	8522	5161	23294	7
4	COI-COII-EF-1 $\alpha$	Equal weights	4/5	9610	8519	5165	23293	5	9610	8519	5165	23293	5
5	COI-COII-EF-1 $\alpha$	Equal weights	5/5	9613	8520	5165	23298	15	9613	8520	5165	23298	15

*Note.* Left half of table refers to trees evaluated with parameters estimated separately for each gene but from a single tree topology (Tree 1). In the last five columns, ML parameters were estimated for each gene independently but also for each individual tree topology.

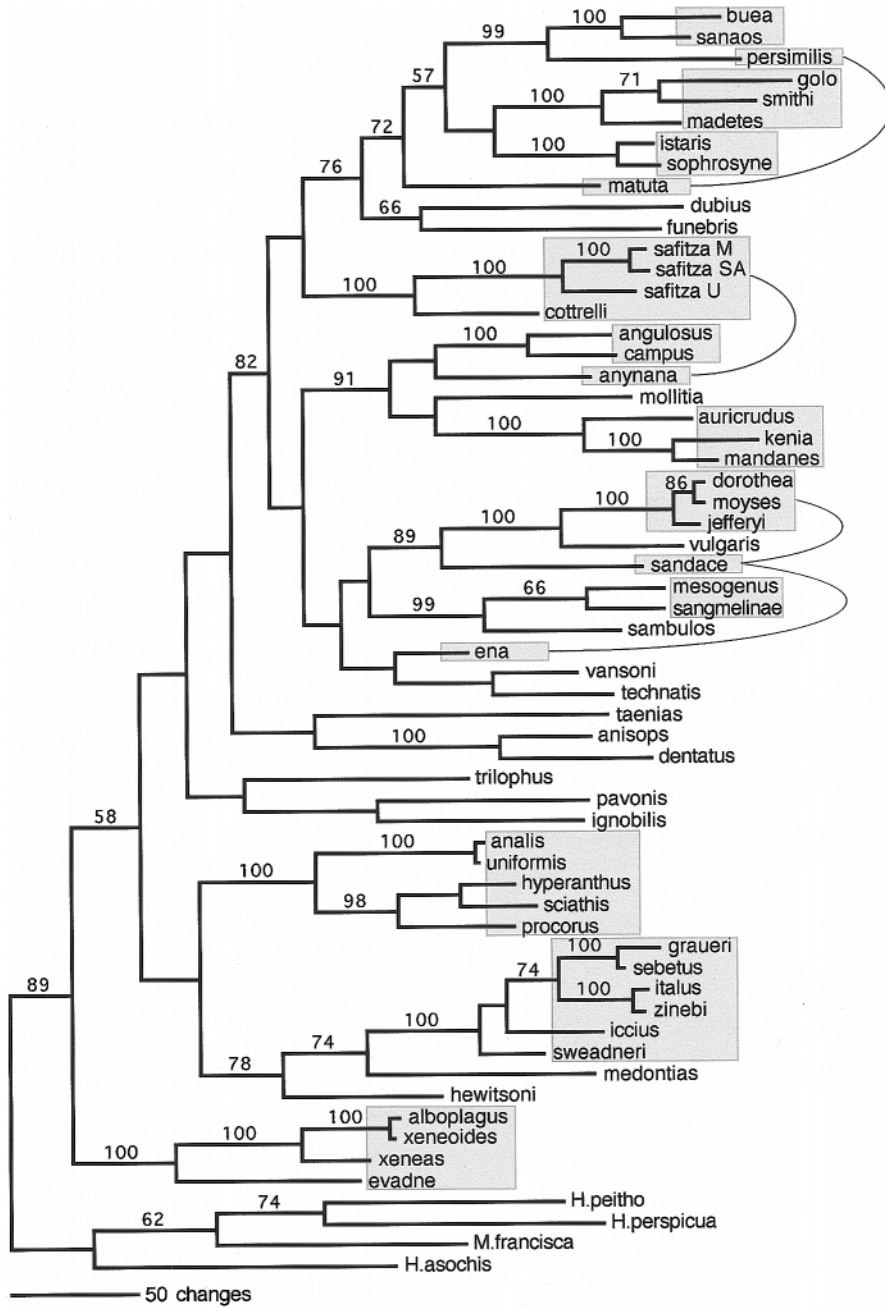


FIG. 4. The first of the five MP trees produced from the combined data with equal weights. Branch lengths and bootstrap values are shown. Shaded blocks as in Fig. 2A.

there was high bootstrap support for *B. vulgaris* to be included within this larger species group (Figs. 1 and 2), we only tested whether *B. ena* could be moved to the base of the *B. dorothea-sandace* clade including *B. vulgaris*.

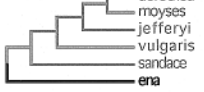

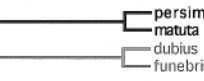
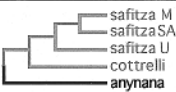

Because *B. ena* was not sequenced in COI and was removed from all tree topologies evaluated under the ML models, we compared these new manually rearranged tree topologies under the total length criteria of MP with equal weights. A Kishino-Hasagawa (1989)

test, implemented in PAUP\*, was performed on tree topologies where only one branch at a time was moved to a new position (Table 9). Tree length increased by 3 steps when *B. ena* was moved to the base of the *B. dorothea-sandace* clade in Tree 4 and by 5 steps in Tree 1. Both these trees were not significantly longer than the shortest trees. All other tree rearrangements produced significantly longer trees.

Our final proposed phylogeny for the genus is based on Tree 4, with the additional *B. ena* branch rearrange-

TABLE 9

Alternative Tree Topologies Created from Manual Branch Rearrangements on Trees 1 and 4 (Fig. 5 displays Tree 1) Were Tested for a Significant Length Difference (under MP) with the Kishino-Hasegawa Test Implemented by PAUP\*

Tree	Length	Length diff.	s.d. (diff.)	t	p
Tree #1 or #4	4559	best			
	4564 (#1)	5	3.60	1.39	0.166
	4562 (#4)	3	2.65	1.13	0.257
	4580 (#1)	21	6.85	3.07	0.002
	4580 (#4)	21	6.85	3.07	0.002
	4583 (#1)	24	6.77	3.55	0.000
	4583 (#4)	24	6.77	3.55	0.000
	4631 (#1)	72	11.32	6.36	0.000
	4585 (#4)	26	7.73	3.36	0.000
	4629 (#1)	70	11.15	6.28	0.000
	4589 (#4)	30	6.91	4.34	0.000

Note. The tree permutations were limited to trying to bring together species belonging to the same species group as defined by Condamin (1973).

ment (Fig. 5). This tree topology has the shortest length (given the rearrangement of *B. ena*) and also brings closer together the clades containing *B. mesogenus*, *B. sangmelinae*, *B. sambulos*, *B. auricrudus*, *B. kenia*, and *B. mandanes*, which Condamin considered close relatives (Fig. 2B). At the morphological level, members of these latter two clades share a marbled type of wing pattern on their ventral surface, which is not found in any other species of the genus (Condamin, 1973). On tree topology 1, to explain the evolution of this wing pattern we would have to hypothesize its occurrence twice whereas in topology 4, only once, with a subsequent loss in the ancestor of the *anynana-mollitia* clade. Also, *B. ena* shares with all the members of the *B. dorothea-sandace* clade a pattern of small dark "ripples" overlying the lighter brown background pigmentation of the wing on the ventral surface. The manual rearrangement of *B. ena* to the base of the *dorothea-sandace* clade makes the "ripples" evolve only once, rather than twice, independently (or alternatively, appear once but be lost twice independently).

With the present molecular data it is difficult to discriminate confidently between the five MP tree topologies, and this is confirmed by the similarity of their

likelihood scores. Strong support for one topology over another may only be achieved by sequencing additional genes. In this study, exhaustive evaluation of the best five MP trees under ML was mostly done for practical purposes since, in future comparative work, we would like to use a single resolved *Bicyclus* tree, rather than a consensus of several trees.

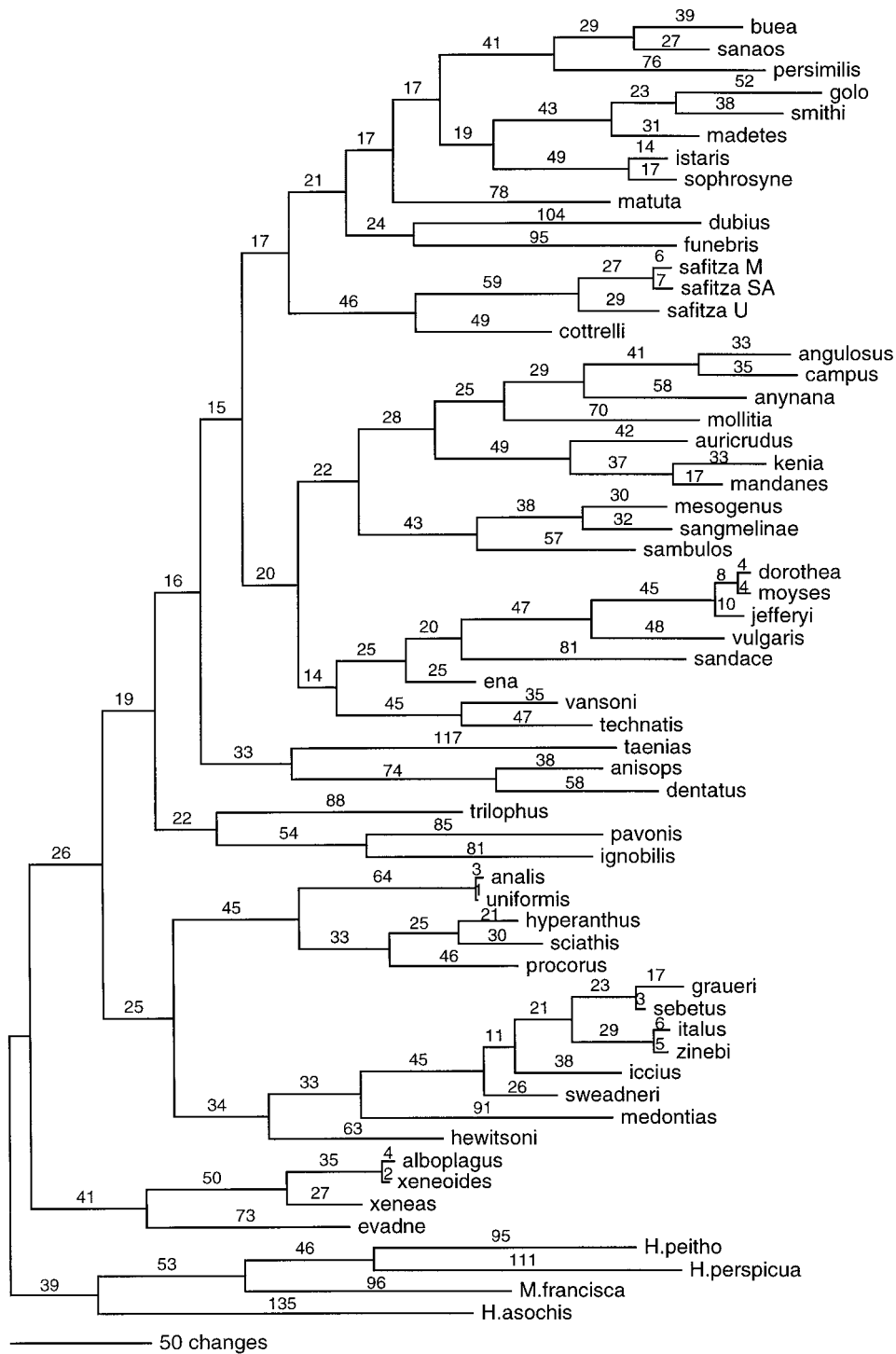
#### Applying a Molecular Clock

We sought to estimate, if only approximately, the historical origin of the clades within the genus *Bicyclus*. We tested whether each mitochondrial gene was evolving under a clock model by taking tree topology of Fig. 5 and computing the likelihood values (with parameters in Table 7) with and without the assumption of rate constancy (Felsenstein, 1988). Twice the difference of the  $-\ln$  likelihood values between the two cases was expected to follow a  $\chi^2$  distribution with  $n - 2$  *df*. Unfortunately, in both cases there was significant rate heterogeneity:  $-\ln$  likelihoods for COI with and without a clock were 10,076.8 and 10,016.9, respectively (LRT = 119.8, *df* = 57,  $P < 0.001$ ) and for COII were 8673.0 and 8630.1 (LRT = 85.9, *df* = 55,  $P = 0.005$ ). For a very approximate dating of the origin of several *Bicyclus* clades, we superimposed the trees for COI and COII, with branch lengths constrained for rate constancy, and assumed a rate of mitochondrial evolution producing 2% sequence divergence for every million years (Desalle *et al.*, 1987; Brower, 1994). With these assumptions, the origin of the *Bicyclus* clade was somewhere between 15 and 20 million years ago (Fig. 6).

## DISCUSSION

It is interesting that despite the high degree of saturation (as measured from the deviations from the  $x = y$  line from the plots of pairwise sequence divergences) found for COI and COII genes relative to EF-1 $\alpha$ , the tree topologies with highest likelihood scores were those produced by a combined MP analysis using equal weights for all positions. This result may come from the fact that the large majority of informative characters for all three genes are rapid (synonymous) changes at third positions and, thus, the best weighting scheme was that which gave these sites a high weight (in this case, equal weight) relative to the other sites. Also, the highest scoring likelihood model will be that which best fits these characters to a topology. Upweighting of putatively more slowly evolving characters, even if less homoplasious, would be unlikely to generate a topology with a higher ML score because most weighted changes would still be from rapidly changing characters.

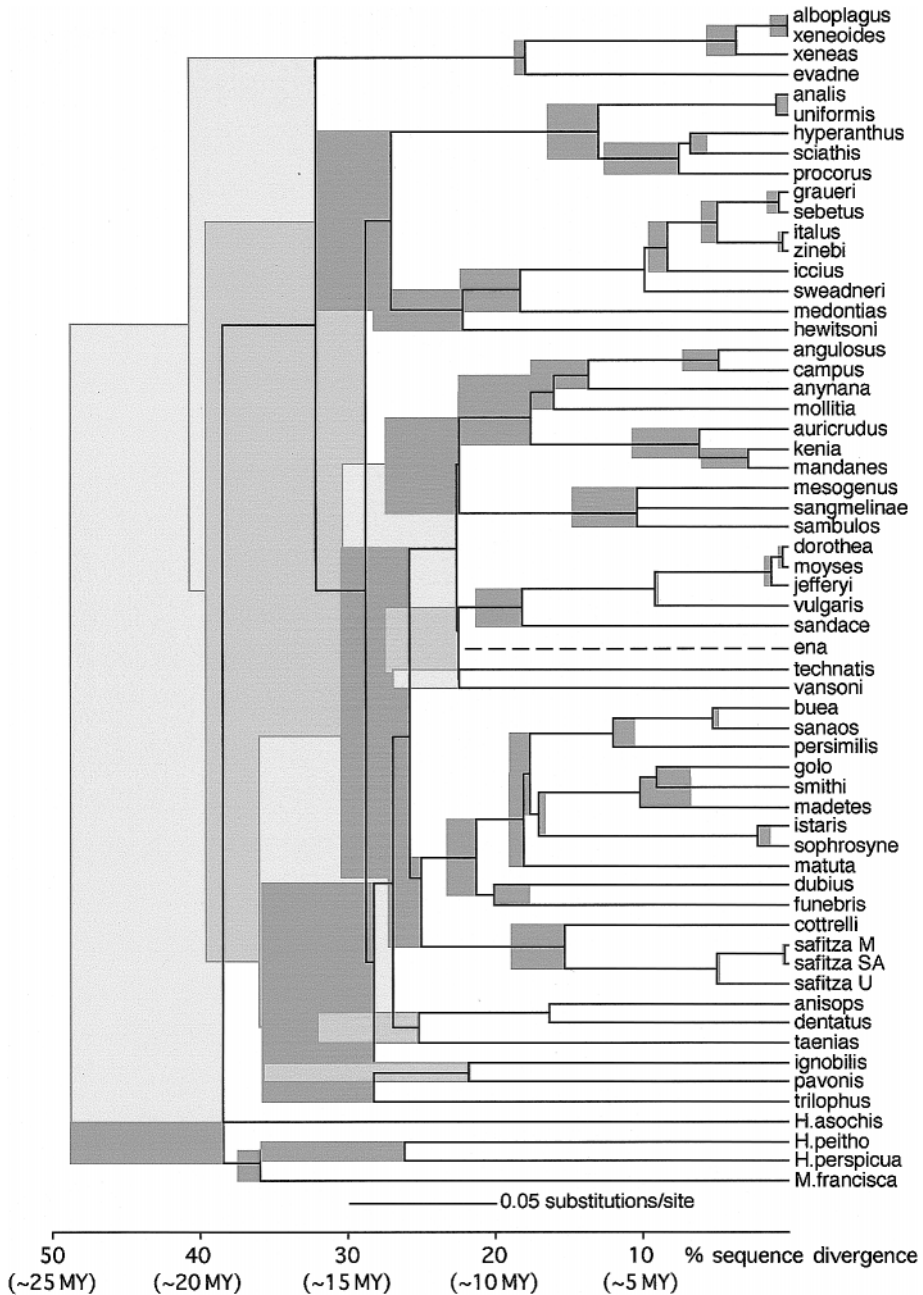
Additionally, the slowly evolving EF-1 $\alpha$  gene was not obviously more useful in sorting older clades within the genus than the faster evolving mitochondrial genes. This finding contrasts with the study of *Papilio* phylogeny by Reed and Sperling (1999), where it was clear



**FIG. 5.** Our chosen *Bicyclus* phylogeny based on Tree 4 (one of the five shortest trees from the MP combined analysis with equal weights) with a manual rearrangement of *B. ena*. Numbers above branches refer to branch lengths.

that EF-1 $\alpha$  was better at resolving basal nodes relative to COI/COII. The discrepancy over the utility of EF-1 $\alpha$  in these two studies may be due to a different age of the genus *Papilio* versus *Bicyclus* or to the more extensive taxon sampling in our study that may have broken

down long branches and improved the resolving power of the faster evolving mitochondrial genes. A simulation study by Yang (1998) concluded that increasing the rate of evolution when it is low greatly improves the accuracy of phylogenetic estimation, but phyloge-



**FIG. 6.** A very approximate estimate of the age of several clades of *Bicyclus*, after forcing a molecular clock to both COI and COII likelihood models of sequence evolution (see Table 6 for model parameters), despite significant rate heterogeneity found between taxa for both genes. The tree topology used was that of Fig. 5. The black lines correspond to the COI clock tree and the shaded boxes represent the alternative branch length for the COII clock tree which is superimposed. The origin of the *Bicyclus* clade was estimated to be between 15 and 20 million years (see text).

netic information is not so easily diluted by extra substitutions. He also concluded that lack of information in sequences of low divergence may be a more serious problem than accumulation of noise in highly divergent sequences. He rejected pairwise sequence divergence as a good indicator of the information content of the data, since the accuracy of phylogeny reconstruction depends not only in the rate of evolution, but also on

how many branches the tree has and how the substitutions are distributed among the branches in the tree. These observations are confirmed by this study.

As already mentioned above, the heavy weighting schemes based on an exact translation of ML rate parameters (first, second, and third position rates as well as  $T_i/T_v$  ratio) to MP weights did very poorly. When partitioning a data set into first, second, and third

positions, and weighting each position with an average weight, no account is taken of particular changes in first positions that result in synonymous substitutions or changes at third positions that result in an amino acid change. When such particular and uncommon cases are weighted with the average weight for the whole partition, biases in tree estimation are likely to occur. Also, this weighting scheme does not take into account areas of faster or slower evolution that are accounted for with the  $\gamma$  parameter in ML. Addition of this parameter when searching for the best model of DNA evolution substantially increased the likelihood of the estimate in all the models tested. The best model found also contained four transversion and two transition classes (the GTR model), rather than just one average rate for transversions and one for transitions. This may explain the relatively poor performance of MP searches using the average  $Ti/Tv$  ratio.

The strategy of weighting all the positions within a gene equally but differently across genes worked well for the study of *Papilio* (Reed and Sperling, 1999), where giving an overall higher weight (five times greater weight) to all the positions of EF-1 $\alpha$  relative to COI and COII overcame some bias of the mitochondrial genes to resolve the more basal nodes incorrectly in a combined analysis. In our study, this weighting scheme produced a tree with a lower likelihood ( $-\ln$  likelihood = 2388) than that for the equally weighted genes. Also, in the *Papilio* study, ML estimates of positional substitution rates for COI, COII, and EF-1 $\alpha$  were substantially different from ours. In particular, the authors found that COI and COII third positions were evolving 16 and 22 times faster relative to EF-1 $\alpha$  third positions, respectively. In our study, COI and COII third positions were only evolving approximately 3 times faster relative to EF-1 $\alpha$  third positions. This discrepancy maybe due to several factors, among which are the way the rates were calculated (from pairs of closely related species versus from the whole data set, using a ML model), the number and sampling of taxa, and actual differences between the rates of nuclear versus mitochondrial genes in the different butterfly genera. In particular, Yang and Yoder (1999) and Sullivan *et al.* (1999) have highlighted that ML estimations of the  $Ti/Tv$  ratio, the  $\gamma$  distribution shape parameter ( $\alpha$ ), and the proportion of invariable sites ( $I$ ) are highly sensitive to taxon sampling. Our estimates of synonymous substitution rates for the mitochondrial and nuclear genes, however, are in good agreement with those found for pairs of closely related species of *Drosophila* (Moriyama and Powell, 1997).

This phylogeny goes beyond just clustering species in groups and presents a fairly well-resolved and supported estimate of how these groups relate to one another. Each gene resolves in a similar way groups at the tips of the tree and there were no major incongruences found among them. When these are combined,

however, several basal nodes become better supported. The ingroup, *Bicyclus*, is well supported as well as the most basal clade within *Bicyclus*, the *B. alboplagus-evadne* clade.

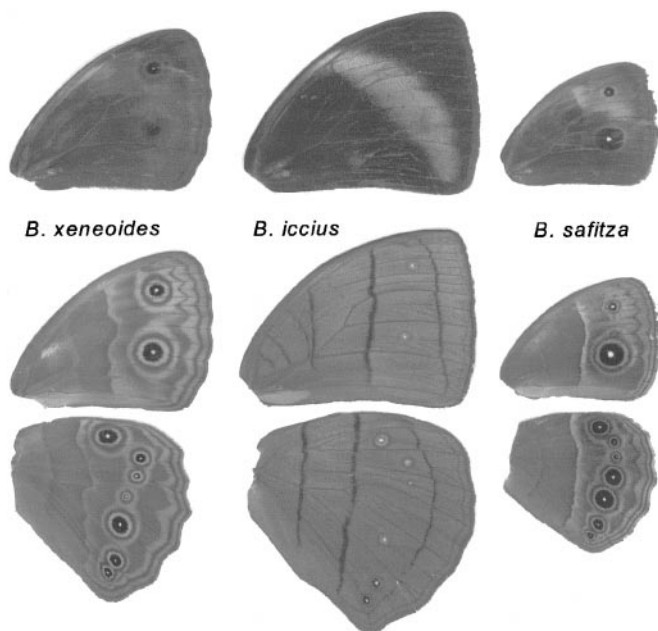
In summary, we believe that the utility of COI and COII is evident in this study. The slower evolving EF-1 $\alpha$  was also useful as an independent gene of nuclear inheritance that showed strong concordance with the grouping of tip species. Together, these genes on the one hand confirmed many of the species groups hypothesized by Condamin (1973) and, on the other, further resolved the relationships among species groups and the phylogenetic history of the whole genus. The approximate dating of the origin of *Bicyclus* (15 to 20 million years ago) also fits in the middle of Miller's broader estimate of 5 to 38 million years (Miller, 1968).

Major differences between our proposed phylogeny and Condamin's relate to: (1) the position of *B. anynana*, which does not seem to be a close relative of *B. safitza* and *B. cottrelli* (A close examination of Condamin's drawings of the male genitalia for these species and for those of *B. campus* and *B. angulosus* suggests that *B. anynana* is indeed a closer relative of these latter two species.); (2) the relationship between *B. persimilis* and *B. matuta*, which are not as close as postulated by Condamin (There is a close resemblance in both male and female genitalia between *B. persimilis* and *B. buea* and *B. sanaos*, but *B. matuta* does not seem to share most of these similarities. Condamin may have put these two species in the same species group due to a similar (convergent) wing pattern consisting of a conspicuous white transversal band present on both dorsal and ventral surfaces.); (3) the placement of *B. vulgaris*, which should not be in a species group of its own since it always fell within the *dorothea* group; and (4) the placement of the *B. alboplagus-xeneoides-xeneas-evadne* species group as the most basal which contrasts with Condamin, who postulated that *B. tainias* and the *B. analis-uniformis-hyperanthus-sciathis-procorus* group were the most basal.

Some species such as *B. ignobilis*, *B. pavonis*, and *B. trilophus* have fairly long branches and their positions are not well supported. A future revision of the *Bicyclus* phylogeny should include other members of the *pavonis* and *trilophus* groups (*ignobilis* is monospecific) to try to break these branches further and possibly improve node support.

Interestingly, the morphologically most distinct group of species, the *B. graueri-hewitsoni* clade, which some authors considered placing in a separate genus (T. Larsen, personal communication), characterized by their large wing size, small ventral eyespots, presence of unique violet or purple dorsal transversal bands (which reflect UV light; C. Forster, unpublished results), and very straight ventral bands to the central symmetry system (see Fig. 7 and Nijhout, 1991, for





**FIG. 7.** Dorsal (top) and ventral wing patterns of a species belonging to a basal clade (*B. xeneoides*) and two other *Bicyclus* species.

butterfly wing pattern nomenclature), seems to be a derived group within *Bicyclus*.

In this paper, we attempted to produce a well-resolved phylogeny estimate for *Bicyclus* that can provide a working framework for future research. In particular, Roskam (manuscript in preparation) is mapping the evolution of plastic responses in ventral wing pattern on the phylogeny. The plasticity in *Bicyclus* species involves mostly coordinated changes in the size of the ventral eyespots and in the levels of conspicuousness of the central band in cohorts emerging at different times of the year. Species that live in tropical forests with small yearly environmental fluctuations, like *B. iccius* and *B. xeneoides* (see specimens in Fig. 7), may show a different degree of plasticity to that of species living in more seasonal forest-savanna ecotones, like *B. safitza* (Fig. 7; Roskam and Brakefield, 1996). The rearing of species in the laboratory, under a range of environmental conditions, from clades showing varying degrees of plasticity in the field, will help evaluate how much plastic response is due to adaptation to local environment and how much due to historical patterns of relatedness.

Monteiro and Enthoven (manuscript in preparation) are looking at the evolution of the relative size of hindwing eyespots (see the difference in the size of the fourth eyespot relative to the other eyespots between *B. xeneoides* and *B. safitza* in Fig. 7) and are using phylogenetically independent contrasts (Felsenstein, 1985) to understand patterns of covariation among all hindwing eyespots and determine the evolutionary lability of individual eyespots or subsets of eyespots.

They propose to explain these patterns of covariation with reference to the underlying developmental organization of the wing, e.g., where covarying eyespots may be sitting in an area of the wing expressing a similar array of "selector genes" laid out early in wing development.

## ACKNOWLEDGMENTS

We thank William Piel, Homer Ntele Allo, Christoph Haag, José Pedro Tavares, Patrícia Salgueiro, and Fausto Abreu, for their assistance in two field trips to collect butterflies. Robert Ducarme, David Lees, Hans Roskam, Paul Brakefield, Steve Collins, and Torben Larsen provided additional specimens of *Bicyclus*. Michel Pieron and Amougou Akoa helped us obtain collecting permits in Cameroon. André Mignault taught A.M. techniques of DNA sequencing and facilitated many aspects of the research. Jen Bush provided logistical support. Mayako Michino, Cara Forster, Jennifer Fines, and Laela Sturdy were supported by Radcliff Science Partners Research grants to assist with the sequencing. Dana Campbell, Belinda Chang, Arne Mooers, Hendrik-Jan Megens, and David Swofford provided advice on the analysis. William Piel, David Lees, Belinda Chang, Arne Mooers, Paul Brakefield, Brian Farrell, Hans Roskam, and an anonymous referee made helpful comments on the manuscript. This research was supported by a Ciência grant to A.M. from Program PRAXIS XXI, Portugal; a Human Frontiers Science Program grant from the European Community; a Milton Fund grant to A.M. and N.E.P. from Harvard University; and the National Science Foundation (DEB-9615760).

## REFERENCES

- Ackery, P. R. (1988). Hostplants and classification: A review of nymphalid butterflies. *Biol. J. Linn. Soc.* **33**: 95–203.
- Aoki, T., Yamaguchi, S., and Uemura, Y. (1982). "Butterflies of the South East Asian Islands. III. Satyridae, Libytheidae." Plapac Co., Ltd., Tokyo.
- Brakefield, P. M. (1996). Seasonal polyphenism in butterflies and natural selection. *Trends Ecol. Evol.* **11**: 275–277.
- Brakefield, P. M. (1998). The evolution-development interface and advances with the eyespot patterns of *Bicyclus* butterflies. *Heredity* **80**: 265–272.
- Brakefield, P. M., and French, V. (1995). Eyespot development on butterfly wings: The epidermal response to damage. *Dev. Biol.* **168**: 98–111.
- Brakefield, P. M., and French, V. (1999). Butterfly wings: The evolution of development of colour patterns. *BioEssays* **21**: 391–401.
- Brakefield, P. M., Gates, J., Keys, D., Kesbeke, F., Wijngaarden, P. J., Monteiro, A., French, V., and Carroll, S. B. (1996). Development, plasticity and evolution of butterfly eyespot patterns. *Nature* **384**: 236–242.
- Brakefield, P. M., and Kesbeke, F. (1997). Genotype-environment interactions for insect growth in constant and fluctuating temperature regimes. *Proc. R. Soc. Lond. B* **264**: 717–723.
- Brakefield, P. M., Kesbeke, F., and Koch, P. B. (1998). The regulation of phenotypic plasticity of eyespots in the butterfly *Bicyclus anynana*. *Am. Nat.* **152**: 853–860.
- Brakefield, P. M., and Reitsma, N. (1991). Phenotypic plasticity, seasonal climate and the population biology of *Bicyclus* butterflies (Satyridae) in Malawi. *Ecol. Entomol.* **16**: 291–303.
- Brower, A. V. Z. (1994a). Phylogeny of *Heliconius* butterflies inferred from mitochondrial DNA sequences (Lepidoptera: Nymphalidae). *Mol. Phylogenet. Evol.* **3**: 159–174.

- Brower, A. V. Z. (1994b). Rapid morphological radiation and convergence among races of the butterfly *Heliconius erato* inferred from patterns of mitochondrial DNA evolution. *Proc. Natl. Acad. Sci. USA* **91**: 6491–6495.
- Caterino, M. S., and Sperling, F. A. H. (1999). Papilio phylogeny based on mitochondrial cytochrome oxidase I and II genes. *Mol. Phylogenet. Evol.* **11**: 122–137.
- Chang, B. S. W., and Campbell, D. L. (2000). Bias in phylogenetic reconstruction of vertebrate rhodopsin sequences. *Mol. Biol. Evol.* **17**: 1220–1231.
- Cho, S., Mitchell, A., Regier, J. C., Mitter, C., Poole, R. W., Friedlander, T. P., and Zhao, S. (1995). A highly conserved nuclear gene for low-level phylogenetics: Elongation factor-1a recovers morphology-based tree for Heliiothine moths. *Mol. Biol. Evol.* **12**: 650–656.
- Clary, D. O., and Wolstenholme, D. R. (1985). The mitochondrial DNA molecule of *Drosophila yakuba*: Nucleotide sequences, gene organization, and genetic code. *J. Mol. Evol.* **22**: 252–271.
- Condamine, M. (1973). "Monographie du genre *Bicyclus* (Lepidoptera, Satyridae)." IFAN, Dakar.
- Desalle, R., Freedman, T., Prager, E. M., and Wilson, A. C. (1987). Tempo and mode of sequence evolution in mitochondrial DNA of Hawaiian *Drosophila*. *J. Mol. Evol.* **26**: 157–164.
- Farris, J. S., Källersjö, M., Kluge, A. G., and Bult, C. (1994). Testing significance of incongruence. *Cladistics* **10**: 315–319.
- Felsenstein, J. (1985). Phylogenies and the comparative method. *Am. Nat.* **125**: 1–15.
- Felsenstein, J. (1988). Phylogenies from molecular sequences: Inference and reliability. *Annu. Rev. Genet.* **22**: 521–565.
- French, V., and Brakefield, P. M. (1992). The development of eyespot patterns on butterfly wings: Morphogen sources or sinks? *Development* **116**: 103–109.
- French, V., and Brakefield, P. M. (1995). Eyespot development on butterfly wings: The focal signal. *Dev. Biol.* **168**: 112–123.
- Kamiie, K., Taira, H., Ooura, H., Kakuta, A., Matsumoto, S., Ejiri, S., and Katsumata, T. (1993). Nucleotide sequence of the cDNA encoding silk gland elongation factor 1 alpha. *Nucleic Acids Res.* **21**: 742.
- Kishino, H., and Hasegawa, M. (1989). Evaluation of the maximum likelihood estimate of the evolutionary tree topologies from DNA sequence data, and the branching order in Hominoidea. *J. Mol. Evol.* **29**: 170–179.
- Larsen, T. (1999). "Butterflies of West Africa—Origins, Natural History, Diversity, and Conservation." CD-Rom (Draft systematic part). Manila.
- Lees, D. C. (1997). "Systematics and Biogeography of Madagascan Mycalesine Butterflies (Lepidoptera: Satyridae)," unpublished Ph.D. thesis. University of London, London.
- Maddison, W. P. (1997). Gene trees in species trees. *Syst. Biol.* **46**: 523–536.
- Maddison, W. P., and Maddison, D. R. (1992). "MacClade," version 3.06. Sinauer, Sunderland, MA.
- Miller, L. D. (1968). The higher classification, phylogeny and zoogeography of the Satyridae (Lepidoptera). *Mem. Am. Entomol. Soc.* **24**: 1–174.
- Mitchell, A., Cho, S., Regier, J. C., Mitter, C., Poole, R. W., and Matthews, M. (1997). Phylogenetic utility of *elongation factor-1a* in Noctuoidea (Insecta: Lepidoptera): The limits of synonymous substitution. *Mol. Biol. Evol.* **14**: 381–390.
- Monteiro, A., Brakefield, P. M., and French, V. (1997a). Butterfly eyespots: The genetics and development of the color rings. *Evolution* **51**: 1207–1216.
- Monteiro, A., Brakefield, P. M., and French, V. (1997b). The genetics and development of an eyespot pattern in the butterfly *Bicyclus anynana*: Response to selection for eyespot shape. *Genetics* **146**: 287–294.
- Monteiro, A., Brakefield, P. M., and French, V. (1997c). The relationship between eyespot shape and wing shape in the butterfly *Bicyclus anynana*: A genetic and morphological approach. *J. Evol. Biol.* **10**: 787–802.
- Monteiro, A. F., Brakefield, P. M., and French, V. (1994). The evolutionary genetics and developmental basis of wing pattern variation in the butterfly *Bicyclus anynana*. *Evolution* **48**: 1147–1157.
- Moriyama, E. N., and Powell, J. R. (1997). Synonymous substitution rates in *Drosophila*: Mitochondrial versus nuclear genes. *J. Mol. Evol.* **45**: 378–391.
- Nei, M., and Gojobori, T. (1986). Simple methods for estimating the numbers of synonymous and nonsynonymous nucleotide substitutions. *Mol. Biol. Evol.* **3**: 418–426.
- Nijhout, H. F. (1991). "The Development and Evolution of Butterfly Wing Patterns." Smithsonian Inst. Press, Washington, DC.
- Pierce, N. E., and Nash, D. R. (1999). The Imperial Blue, *Jalmenus evagoras* (Lycaenidae), In "The Biology of Australian Butterflies" (R. Kitching, E. Sheermeyer, R. Jones, and N. E. Pierce, Eds.), Monographs in Australian Lepidoptera, Vol. 6, pp. 277–316. CSIRO Press, Sydney.
- Rand, D. B., Heath, A., Suderman, J., and Pierce, N. E. (2000). Phylogeny and life history evolution of the genus *Chrysoritis* within the Aphnaeini (Lepidoptera: Lycaenidae) inferred from mitochondrial *cytochrome oxidase I* sequences. *Mol. Phylogenet. Evol.* **17**: 85–96.
- Reed, R. D., and Sperling, F. A. H. (1999). Interaction of process partitions in phylogenetic analysis: an example from the swallowtail butterfly genus *Papilio*. *Mol. Biol. Evol.* **16**: 286–297.
- Roskam, J. C., and Brakefield, P. M. (1996). A comparison of temperature-induced polyphenism in African *Bicyclus* butterflies from a savannah-rainforest ecotone. *Evolution* **50**: 2360–2372.
- Saccheri, I. J., Brakefield, P. M., and Nichols, R. A. (1996). Severe inbreeding depression and rapid fitness rebound in the butterfly *Bicyclus anynana* (Satyridae). *Evolution* **50**: 2000–2013.
- Saccheri, I. J., Wilson, I. J., Nichols, R. A., Bruford, M. W., and Brakefield, P. M. (1999). Inbreeding of bottlenecked butterfly populations: Estimation using the likelihood of changes in marker allele frequencies. *Genetics* **151**: 1053–1063.
- Sullivan, J., Swofford, D. L., and Naylor, G. J. P. (1999). The effects of taxon sampling on estimating rate heterogeneity parameters of maximum-likelihood models. *Mol. Biol. Evol.* **16**: 1347–1356.
- Swofford, D. L. (1998). "PAUP\*: Phylogenetic Analysis Using Parsimony (\*and Other Methods)," version 4.0b2a. Sinauer, Sunderland, MA.
- Swofford, D. L., Olsen, G. J., Waddell, P. J., and Hillis, D. M. (1996). Phylogenetic inference. In "Molecular Systematics" (D. M. Hillis, C. Moritz, and B. K. Mable, Eds.), pp. 407–514. Sinauer, Sunderland, MA.
- Windig, J. J., Brakefield, P. M., Reitsma, N., and Wilson, J. G. M. (1994). Seasonal polyphenism in the wild: Survey of wing patterns in five species of *Bicyclus* butterflies in Malawi. *Ecol. Entomol.* **19**: 285–298.
- Yang, Z. (1998). On the best evolutionary rate for phylogenetic analysis. *Syst. Biol.* **47**: 125–133.
- Yang, Z., Goldman, N., and Friday, A. E. (1994). Comparison of models for nucleotide substitution used in maximum likelihood phylogenetic estimation. *Mol. Biol. Evol.* **11**: 316–324.
- Yang, Z. H., and Yoder, A. D. (1999). Estimation of the transition/transversion rate bias and species sampling. *J. Mol. Evol.* **48**: 274–283.